

# Statistical Analysis of Coastal Currents from HF Radar Along the North-Western Bay of Bengal



Samiran Mandal, Saikat Pramanik, Subrota Halder and Sourav Sil

**Abstract** Highly accurate ocean current measurements are very much important in the field of ocean engineering. Over the past decades, the High-Frequency (HF) Radars are known to be one of the important marine instruments for oceanographic studies. The present work focuses mainly on statistical analysis of HF radar-measured ocean surface current along the Odisha coast, north-western Bay of Bengal during 2015. The observations indicate that northward propagating Western Boundary Current (WBC) and southward propagating East India Coastal Current (EICC) can reach up to 1.8 m/s and 1.0 m/s, respectively. The zonal (meridional) components vary in the range  $-0.8$  to  $0.8$  ( $-0.6$  to  $0.7$ ) m/s along with standard deviation of 0.25 m/s for both the components with 99% significance level. The boxplot analysis shows the extreme values of both the zonal and meridional currents along with the negative medians; however, certain outliers are observed only for zonal currents. The 25th percentile is less than  $-0.20$  m/s for the meridional currents, whereas opposite result for zonal currents. The zonal and meridional currents follow normal distribution, whereas the current magnitude and kinetic energy follow Weibull distribution. The Weibull shape parameter ( $\beta$ ) varies for both the parameters: current magnitude ( $\beta > 1$ ) and kinetic energy ( $0 < \beta < 1$ ) due to the variations in moments, which indicates that in case of kinetic energy (current magnitude), the failure rate decreases (increases) over time. This circulation variability can be attributed predominantly to the winds and the coastal dynamics.

**Keywords** Bay of Bengal · HF radar · Ocean currents · Statistics and tides

---

S. Mandal (✉) · S. Pramanik · S. Halder · S. Sil  
School of Earth, Ocean and Climate Sciences, Indian Institute of Technology Bhubaneswar,  
Bhubaneswar, India  
e-mail: [samiranmandal7@gmail.com](mailto:samiranmandal7@gmail.com)

S. Halder  
Indian Institute of Tropical Meteorology, Pune, India

© Springer Nature Singapore Pte Ltd. 2019  
K. Murali et al. (eds.), *Proceedings of the Fourth International Conference in Ocean Engineering (ICOE2018)*, Lecture Notes in Civil Engineering 23,  
[https://doi.org/10.1007/978-981-13-3134-3\\_8](https://doi.org/10.1007/978-981-13-3134-3_8)

## 1 Introduction

Over the past two decades, the High-Frequency (HF) radars are known to be one of the important marine instruments for oceanographic studies and thereby have proved to be the most efficient instrument for measuring ocean surface currents along the coast. The high-frequency datasets provide us the opportunity for multi-scale analysis of ocean surface currents along the coastal regions. The Bay of Bengal (BoB), covering the north-eastern part of the Indian Ocean ( $76^{\circ}$ – $100^{\circ}$ E,  $4^{\circ}$ – $24^{\circ}$ N), is a semi-enclosed tropical ocean basin. The current system on the western boundary in the BoB is well known for its unique circulation pattern with high complexity as compared to the rest of the basin. The space–time current variability, northward during spring and southward during autumn, has been studied from various hydrographic datasets [1], satellite altimetry datasets [2–4] and numerical simulations [5–7] in the past few decades. Earlier circulation studies were mostly basin scale and from ocean models and satellites. The observational data are limited along the Indian coast of the BoB, till Earth System Science Organization—National Institute of Ocean Technology (ESSO-NIOT), Indian National Centre for Ocean Information Services (ESSO-INCOIS) have installed five pairs of the long-range SeaSonde HF Radar systems along the Indian coastline, operating continuously since 2009, in order to remotely sense the ocean surface currents covering the coastal regions of India [8]. Specifically, we focus on the HF radar datasets (4.8 MHz) installed along the Odisha coast (from Puri and Gopalpur stations) that is available (courtesy: INCOIS) hourly on a 6-km grid (albeit with spatial and temporal gaps) over a limited region ( $18$ – $20$  N,  $85$ – $87$  E) (Fig. 1). The current observations from HF radar and their statistical distribution are the new findings of this study.

The HF Radars can be used for real-time ocean monitoring and ocean state forecasting purposes through the numerical simulations. Among the implications, one of the major implications is the efficient management of coastal hazards. Also, the HF Radar-derived surface currents maps enable to improve the navigation for safety purposes in the restricted areas (ports and harbours). The finer temporal variability of the surface currents enables Lagrangian tracking of small parcels of surface water, which enables hazard mitigation in managing suspended sediments in dredging, in emergency situations where flotsam and other drifting items need to be found, and in pollution control. Nowadays, the real-time tsunami monitoring is also provided by the HF Radars. Inspired by all these, the present study focuses primarily on the statistical analysis of the coastal currents in 2015 along the north-western BoB.

The structure of the paper is as follows; a brief description of Weibull distribution is given in Sect. 2. The data and methodology are discussed in Sect. 3, the results and discussions are described in Sect. 4, and finally, the conclusions are reported in Sect. 5 followed by acknowledgements and a list of references.

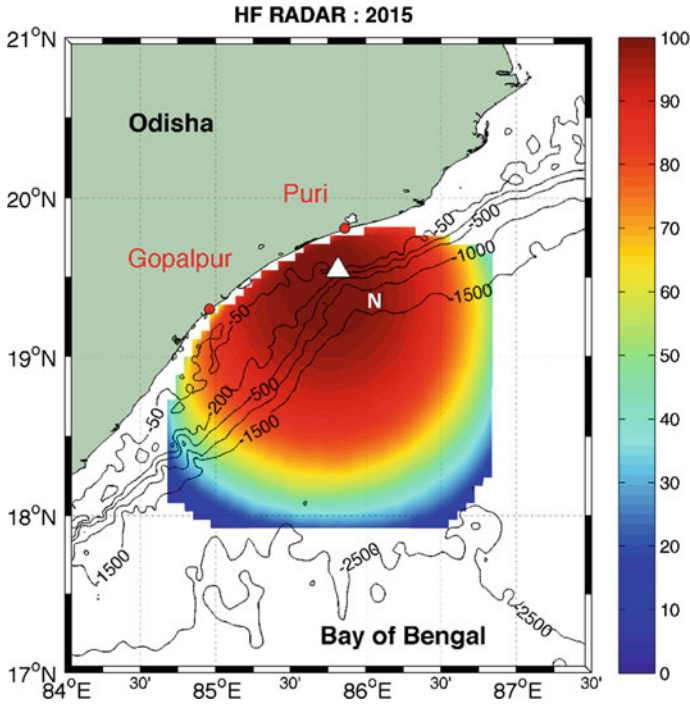


**Fig. 1** The data coverage (shaded) during 2015 in percentage (%). The location at nearshore ‘N’ is indicated by the triangle symbol. Black contours denote the isobaths of –50, –200, –500, –1000, –1500 and –2500 m. The red dots are the HF Radar stations along Odisha coast

## 2 Weibull Distribution

The Weibull probability density function (PDF) is defined only for all positive values,  $x > 0$ , as

$$f(x; k, \lambda) = \frac{\beta}{\lambda} \left(\frac{x}{\lambda}\right)^{\beta-1} e^{-(x/\lambda)^\beta}$$

where  $\lambda$  and  $\beta$  are the two positive parameters. The term  $\lambda$  is the scale parameter of the distribution, and  $\beta$  is the shape parameter. Many studies have indicated that the distribution of wind speed can be represented by the Weibull distribution [9]. Depending on the values of the parameters, the Weibull distribution can be used to model weather forecasting. In this study, we will examine how the values of the shape parameter,  $\beta$ , and the scale parameter,  $\lambda$ , affect such distribution characteristics, like, the shape of the curve, the reliability, and the failure rate. Note that in the rest of this paper, the general form of Weibull distribution (2 parameters) has been assumed.

### 3 Data and Methodology

The measurements of high radar frequency echoes backscattered from the sea surface can be used to deduce information on both waves and surface currents. These radars are of direction finding type, consisting of one receiving and one transmitting antennae at each of the locations. The two radars at the Odisha coast which are located at Gopalpur (84.96°E, 19.30°N) and the other at Puri (85.86°E, 19.80°N) covers a region of ~200 km from the coast [8], the locations are shown in Fig. 1. The high resolution (~6 km) and high-frequency (hourly) surface current from HF Radar during 2011 (source: INCOIS, India) along the Odisha coast is initially used for this analysis. The daily winds derived from ASCAT are used with 25 km × 25 km spatial resolution, provided by IFREMER, France due the concurrent period of HF Radar data availability.

The current time series at the location with maximum data availability is chosen for the analysis. The basic statistics (standard deviation, median, probability distribution function) have been derived with the help of box plots, frequency distribution curves, via, kernel distribution estimation. In addition, the surface current variability has also been analysed along the north-western BoB.

### 4 Results and Discussions

A thorough statistical analysis has been carried out at location N (with maximum data availability). The statistical metrics include the standard measures of centre (mean, mode and median) and dispersion (range and standard deviation), student's t-test, kernel distribution estimation. In addition, both the higher frequency variability as well as daily variability has also been analysed. This section is divided into two parts with focuses statistical analysis and daily variability of the currents.

#### 4.1 Variability of Coastal Currents

The HF Radar datasets are important to explain the higher resolution sub-mesoscale features which are not even resolved by the models. So, the main focus of this section is the ability of the radars to capture the oceanic and associated coastal processes. The validation of the surface currents on daily scale has already been carried out using OSCAR (satellite-derived currents) and HYCOM (model-simulated currents) currents, as no other in situ observations are available in this domain [10].

The southward flow is usually observed during the months of January, but in 2015 the southward flow persisted till mid of February. However, the reversal phase is observed from February end, which indicates the formation of the northward Western Boundary Current (WBC). Northward currents are strong with an amplitude of

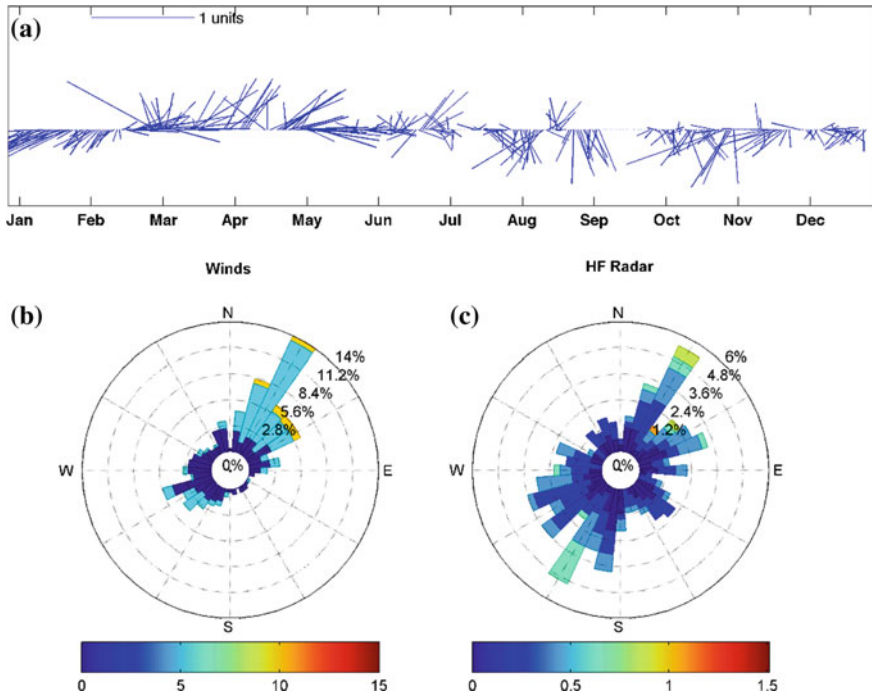


**Fig. 2** a The current direction and magnitudes in m/s (sticks) for HF radar (upper panel) at location N for the year 2015. The lower panel shows the rose plots for **b** winds and **c** HF radar currents

1.8 m/s (Fig. 2a). However, the reversal of currents is again observed during July and the intensified southward propagating EICC is observed during October–November 2015 (Fig. 2a). The current magnitude of 1.2 m/s is observed during this period, as compared to the springtime WBC. This reversal is caused mainly due to the reversal of the winds. In addition, the present year is rich with eddy variability and propagated along the coastline (Fig. 2a), which may be due to interaction with the coastal topography (Fig. 1). It is surprising to note that the WBC in its intensified stage is observed very nearby the coastline. The rose plot for the surface currents (Fig. 2b) and the winds (Fig. 2c) indicate that the north-eastward and south-westward circulation patterns are generally forced by the winds, whereas the other variability observed in the circulation pattern is expected to be due to the local coast and continental shelf dynamics. The detailed analysis will be carried out in the nearby future.

## 4.2 Statistical Analysis of Coastal Currents

Since the main focus of the work is the statistical analysis of the HF radar-derived surface currents, so the following statistical results have been derived. The zonal

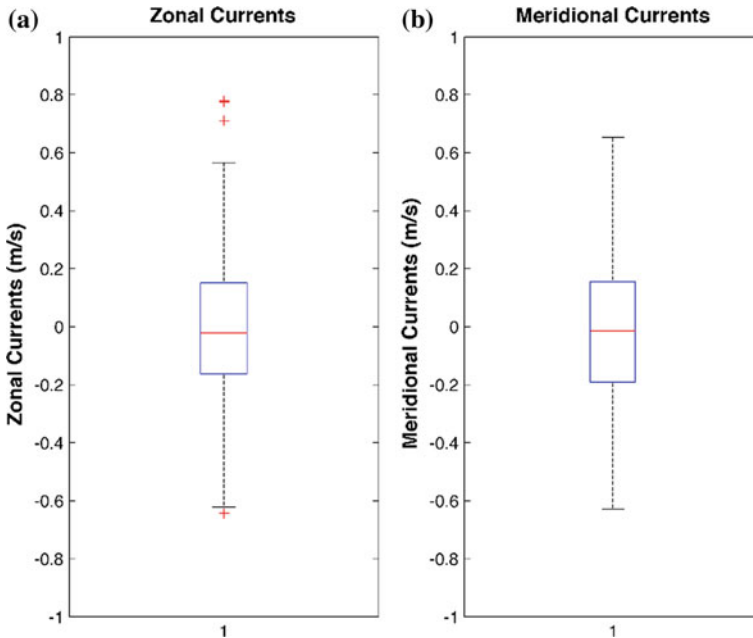


**Fig. 3** The boxplots for **a** zonal and **b** meridional currents at the location N. The red plus marks are the whiskers. The red line in the middle of the box is the median. The upper (lower) end of the box indicates the third (first) quartile

component and meridional components vary in the range  $-0.8$  to  $0.8$  m/s and  $-0.6$  to  $0.7$  m/s, respectively (Fig. 3). The mean current is negative for the entire year, however, the sometimes currents are clearly positive, specifically during the following three periods: mid-February to May, August and December. Very low standard deviation of  $0.25$  m/s is observed for both the components. The boxplot analysis shows extreme values of both the zonal and meridional currents along with the negative medians; however, certain outliers are observed only for zonal currents (Fig. 3).

The 25th percentile is less than  $-0.2$  m/s for the meridional currents, whereas opposite result for zonal currents. The interquartile range is observed more for meridional component indicating more variability. However, the variability will be observed more in case of the box analysis is done on the monthly basis. Also, student's t-test shows that the null hypothesis is rejected and that the mean of the data is significantly different from zero, with 99% significance level.

Finally, both the velocities components (zonal and meridional), current magnitude and kinetic energy are analysed through the kernel distribution estimation, i.e. the probability distribution functions are determined. The zonal and meridional currents follow a normal distribution (Fig. 4a, b) whereas, the current magnitude and kinetic energy follow Weibull distribution (Fig. 4c, d). In case of ocean surface currents derived from HF Radars, the shape parameter ( $\beta$ ) varies for both the quantities:

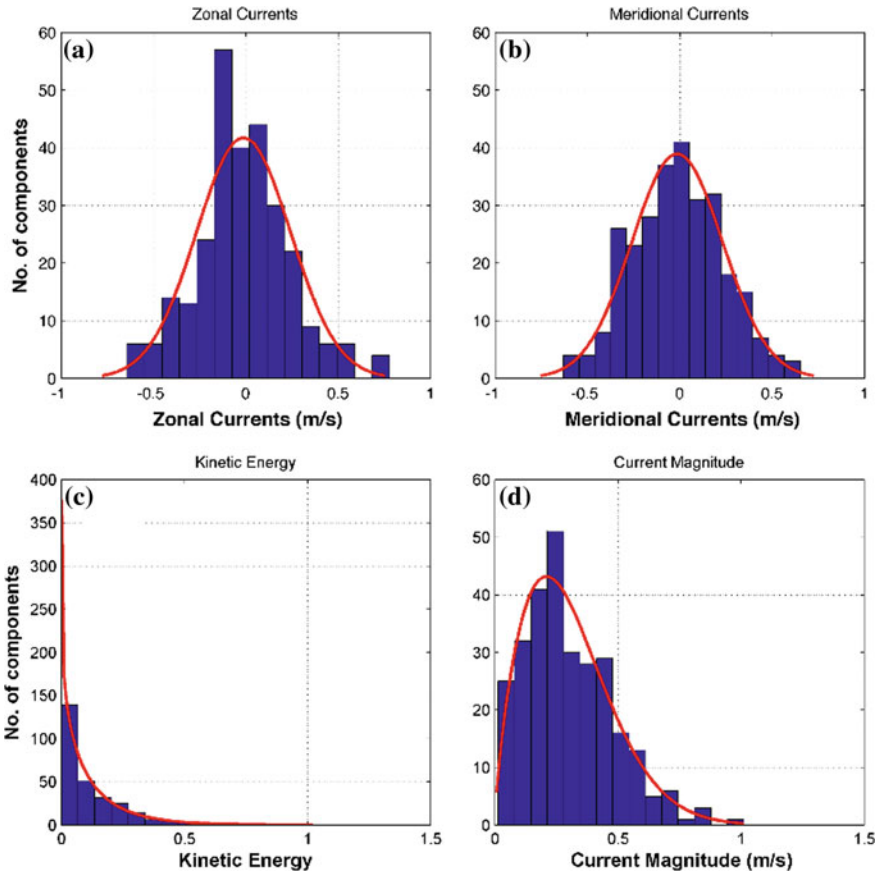


**Fig. 4** The probability density functions of the time series at location N for **a** zonal currents (m/s) **b** meridional currents (m/s) **c** kinetic energy (m<sup>2</sup>/s<sup>2</sup>) and **d** current magnitude (m/s)

the value is 1.74 for current magnitude (i.e.  $\beta > 1$ ) and 0.87 for kinetic energy (i.e.  $0 < \beta < 1$ ) due to the variations in moments (Fig. 4c, d). On the other hand, the scale parameter ( $\lambda$ ) varies for both the quantities as, 0.3 and 0.12 for current magnitude and kinetic energy, respectively (Fig. 4c, d). For a value of  $0 < \beta < 1$ , the failure rate decreases over time. This happens if there is significant ‘infant mortality’, or abstract values are detected early and the failure rate decreases over time as the abstract values are discarded of the population. For a value of  $\beta > 1$ , the failure rate increases with time. This happens if there is an ‘aging’ process, or parts that are more likely to fail as time goes on. So, shape parameter ( $\beta$ ) analysis indicates that in the case of kinetic energy the failure rate decreases over time, whereas in the case of current magnitude, the failure rate increases over time.

The main driving force of surface currents seems to be the wind forcing in the open ocean whereas, nearby the coastline it is driven both by the winds and coastal

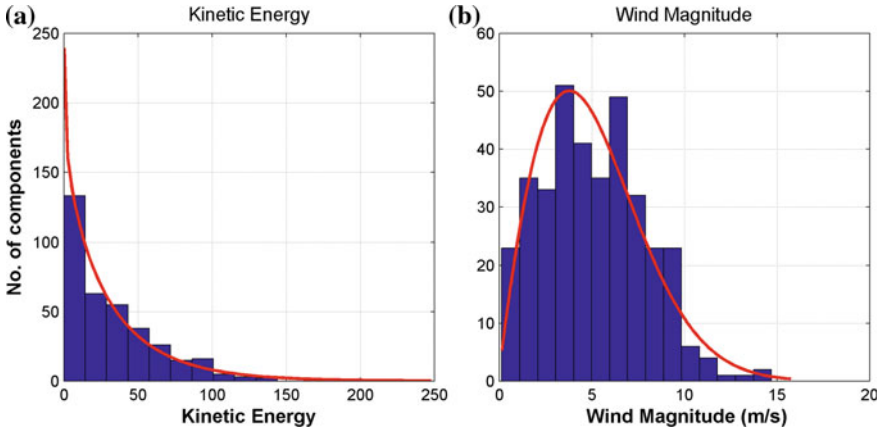


**Fig. 5** The probability density functions of the time series at location N for **a** kinetic energy ( $\text{m}^2/\text{s}^2$ ) and **b** wind magnitude (m/s) of winds from ASCAT

dynamics. To obtain the relationship with the wind, similar distribution analysis has been carried out with winds at the same location. The shape parameter ( $\beta$ ) varies for both the quantities: the value is 1.86 for wind magnitude and 0.93 for kinetic energy due to the variations in moments (Fig. 5a, b). On the other hand, the scale parameter ( $\lambda$ ) varies for both the quantities as, 5.71 and 32.65 for wind magnitude and kinetic energy, respectively (Fig. 5a, b). The results from the analysis of the winds are consistent with those of the surface currents (Fig. 2b, c). So, the variability in the circulation pattern can be attributed to the variability in the wind pattern. The presence of lots of gap in the current datasets for the year 2015 restricts our study to daily scale, so high-frequency variability will be checked once the gap filling is done. The tidal analysis with carried out in future to aid the knowledge of the tidal driven current in this region via, ADCPs [11] and tide gauge datasets [12].

## 5 Conclusions

The study indicated the usability of the statistics derived from the HF radar datasets in this domain, via, their statistical analysis. The northward propagating WBC and southward propagating EICC can reach up to 1.8 m/s and 1.0 m/s, respectively during 2015. The zonal component and meridional components vary in the range  $-0.8$  to  $0.8$  m/s and  $-0.6$  to  $0.7$  m/s, respectively. The mean current is negative for the entire year, however, the currents are clearly positive, during pre-monsoon (May) and post-monsoon (August) period, with a low standard deviation of 0.25 m/s for both components of currents. The analysis shows the extreme values of both the zonal and meridional currents along with the negative medians; however, certain outliers are observed only for zonal currents. The 25th quartile is less than  $-0.2$  m/s



for the meridional currents, whereas the opposite result for zonal currents. Also, student's t-test shows that the null hypothesis is rejected and that the mean of the data is significantly different from zero, with a 99% significance level.

The current/wind magnitude as well as the kinetic energy (for both current and wind) follows a Weibull distribution, which indicates that in case of kinetic energy the failure rate decreases over time, whereas in case of the current magnitude, the failure rate increases over the time. Hence the variability in the circulation pattern is attributed to the variability of the winds. This statistical study will be helpful for engineering purposes as well as ocean state forecasting purposes through numerical simulations. The study also gives an insight of the coastal circulation on the Odisha coast, as it captured the basin scale as well the mesoscale oceanic processes.

**Acknowledgements** We acknowledge the financial support given by the ESSO-INCOIS, Ministry of Earth Sciences (MoES), and Science and Engineering Research Board (SERB) of Department of Science and Technology (DST), Government of India. Also, we sincerely thank Coastal and Environmental Engineering Group, NIOT, Chennai for constant monitoring of the HF Radars and making the data availability efficient. We also acknowledge IITBBS for providing the research facility.

## References

1. Babu MT, Sarma YVB, Murty VSN, Vethamony P (2003) On the circulation in the Bay of Bengal during northern spring inter-monsoon (March–April 1987). *Deep Sea Res Part II* 5:855–865
2. Somayajulu YK, Murty VSN, Sarma YVB (2003) Seasonal and inter-annual variability of surface circulation in the Bay of Bengal from TOPEX/Poseidon altimetry. *Deep-Sea Res I* 50:867–880
3. Durand F, Shankar D, Birol F, Shenoj SSC (2009) Spatio-temporal structure of the East India Coastal Current from satellite altimetry. *J Geophys Res* 114:C02013
4. Gangopadhyay A, Bharat Raj GN, Chaudhuri AH, Babu MT, Sengupta D (2009) On the nature of meandering of the springtime western boundary current in the Bay of Bengal. *Geophys Res Lett* 40:2188–2193
5. Shankar D, McCreary JP, Han W, Shetye SR (1996) Dynamics of the East India Coastal Current: 1. Analytic solutions forced by interior Ekman pumping and local alongshore winds. *J Geophys Res* 101(C6):13975–13991
6. Vinayachandran PN, Kagimoto T, Masumoto Y, Chauhan P, Nayak SR, Yamagata T (2005) Bifurcation of the East India Coastal Current east of Sri Lanka. *Geophys Res Lett* 32:L15606
7. Sil S, Chakraborty A, Ravichandran M (2011) Numerical simulation of surface circulation features over the Bay of Bengal using regional ocean modeling system. *Adv GeoSci* 24:117–130
8. John M, Jena BK, Sivakholundu KM (2015) Surface current and wave measurement during cyclone Phailin by high frequency radars along the Indian coast. *Curr Sci* 108(3):405–409
9. Monahan AH (2006) The probability distribution of sea surface wind speeds. Part I: Theory and SeaWinds observations. *J Clim* 19:497–520
10. Mandal S, Sil S (2017) Coastal currents from HF radars along Odisha Coast. *Ocean Dig Q Newsl Ocean Soc India* 4:112
11. Jithin AK, Unnikrishnan AS, Fernando V, Subeesh MP, Fernandes R, Khalap S, Narayan S, Agarvadekar Y, Gaonkar M, Tari P, Kankonkar A, Verneka S (2017) Observed tidal currents on the continental shelf off the east coast of India. *Cont Shelf Res* 141:51–67
12. Murty TS, Henry RF (1983) Tidal harmonics in the Bay of Bengal. *J Geophys Res* 88(C10):6069–6076